RSC Advances

PAPER

View Article Online
View Journal | View Issue

Cite this: *RSC Adv.*, 2017, **7**, 20537

An azo-phenol derivative probe: colorimetric and "turn-on" fluorescent detection of copper(II) ions and pH value in aqueous solution

Yanchun Li,[a] Xiaojun Han [b] and Yan Song *[c]

Received 25th January 2017
Accepted 31st March 2017

DOI: 10.1039/c7ra01109a

rsc.li/rsc-advances

The optical properties of a novel, rhodamine-based derivative, synthesized by reacting rhodaminehydrazide and an azo-phenol derivative in ethanol, were investigated in ethanol–water solution. The novel sensor displayed selectivity for Cu^{2+} ions, as evidenced by a colourless to dark red colour change, which was characterized using UV visible spectroscopy and which also allowed visual detection of Cu^{2+}. In contrast, selectivity towards pH was determined from changes in the absorption spectra in the micromolar range. This represents the first reported rhodamine-based sensor capable of detecting both Cu^{2+} and pH using two different modes. In addition, the rhodamine-based sensor has been successfully applied in the biomedical research field to the fluorescence imaging of Cu^{2+} in HeLa cells.

1. Introduction

Cu^{2+} has caused serious harm to the environment and human health. It can cause serious injury to human kidneys, lungs, bone and the nervous system, which results in renal dysfunction, calcium metabolism disorders and an increased incidence of certain forms of cancer.[1] However, the mechanisms involved in Cu^{2+}-uptake and carcinogenesis remain undefined.[2,3] The EPA (United States Environmental Protection Agency) gives an enforceable drinking water standard for Cu of 5 ppb to prevent kidney damage and other related diseases, while the WHO (World Health Organization) provides a more strict guideline value for Cu of 3 ppb for drinking water. Therefore, developing reliable methods for Cu^{2+} trace quantification in environmental samples and in living cell/tissue samples is of great significance for clarifying Cu^{2+}-carcinogenesis and other biological effects.

In recent years, the development of fluorescent chemosensors for sensing and reporting heavy transition-metal ions has been receiving considerable attention.[4,5] Fluorescence techniques have become powerful tools for sensing and imaging metal ions in trace amounts because of its simplicity, high sensitivity and real-time monitoring with in short response time. Sensitive and reliable fluorescent molecular sensors seem to be the ideal tool for evaluating and dynamically mapping the intracellular fluctuations of metal ions by using microscopy techniques to allow real-time local imaging.[6–11] Up to now, many fluorescent sensors for Cu^{2+} have been reported,[12,13] but only a few of them are applicable to cellular imaging,[14,15] their practical application is still restrained due to their poor water solubility, UV-excitation and pH-dependent fluorescence in physiological environments. To date, it is still a tremendous challenge to design Cu^{2+}-selective sensors, in particular, fluorescent chemosensor for the accurate detection of Cu^{2+} in aqueous solutions and biological environments.

A practical fluorescent chemosensor must produce a strong fluorescent response upon binding the analyte. Rhodamine, as a dye, is an ideal mode for construction of fluorogenic-labeling and fluorescent chemosensors because of their particular spirolactam structures and excellent photophysical properties, including high absorption coefficient, high fluorescence quantum yield and high photostability.[16,17] By virtue of these fascinating properties, the excellent examples of rhodamine-based fluorescent chemosensor have been designed and successfully applied for detecting metal ions.[18–23] And most rhodamine-based chemosensors are fluorescence enhancement, which is of great importance for metal ions detection.[24,25] Nevertheless, there is a relatively few reports concerned the chemosensor based on rhodamine derivative for selective detection of metal ions in aqueous and application in cell imaging.[26–28]

In this paper, we report the synthesis and fluoroionophoric properties of a novel fluorescent sensor aimed at the selective recognition of Cu^{2+} ions in aqueous solution and living cells. Sensor 1 is composed of an rhodamine fluorophore and a receptor of the *N*,*N*′-bis(salicylidene)-diethylenetriamine attached *via* a space linker. Sensor 1 exhibits Cu^{2+}-selective TURN-ON and Cu^{2+}-selective TURN-OFF type signaling behaviors that can be used to distinguish Cu^{2+} ions. Moreover, to the best of

[a]*Department of Chemistry and Pharmaceutical Engineering, Jilin Institute of Chemical Technology, Jilin, 132022, People's Republic of China*

[b]*State Key Laboratory of Urban Water Resource and Environment, School of Chemistry and Chemical Engineering, Harbin Institute of Technology, 92 West Da-Zhi Street, Harbin, 150001, China*

[c]*Department of Chemical and Materials Engineering, Jilin Institute of Chemical Technology, Jilin, 132022, People's Republic of China. E-mail: songyan199809@163.com*

our knowledge, this is the first example of a cation-induced TURN-ON and TURN-OFF type of fluorescent signal control behavior which was applied to intracellular imaging of Cu^{2+}.

2. Experiment section

2.1 Materials

Rhodamine B 98% purity, (Beijing Hengyue Zongyuan Chemical CO., LTD). *N*,*N*-Dimethylform amide (DMF) was distilled and dried by anhydrous magnesium sulfate. Aniline (99% purity), salicylaldehyde, hydrazine hydrate, and all other reagents were purchased from Sinopharm Chemical Reagent Co., Ltd., and used as received. The solutions of metal ions were prepared from NaCl, KCl, $CaCl_2$, $MgSO_4$, $FeCl_3$, $Mn(NO_3)_2 \cdot 6H_2O$, $CoCl_2 \cdot 6H_2O$, $NiCl_2 \cdot 6H_2O$, $Zn(NO_3)_2$, $CuCl_2$, $CuCl_2 \cdot 2H_2O$, $Hg(NO_3)_2$, $AgNO_3$, $Pb(NO_3)_2$, respectively, and were dissolved in deionized water. Aqueous Tris–HCl (0.1 mol L^{-1}) solution was used as buffer to keep pH value (pH = 7.14), and to maintain the ionic strength of all solutions in experiments.

2.2 Characterization

The synthesis of sensor 1 is shown in Scheme 1. The intermediate, compound (1), was synthesized from salicylaldehyde and aniline following a literature procedure.[29] Compound (2) was prepared in 50.8% yield of pure product by coupling Rhodamine B with hydrazine hydrate. Sensor 1 was easily synthesized by compound (1) and (2) in 75.6% yield, and characterized by ESI-MS, ^{1}H-NMR and ^{13}C-NMR.

^{1}H NMR spectra were measured on a Bruker AV-300 spectrometer with chemical shifts reported as parts per million (in $CDCl_3$, TMS as internal standard). IR spectra were recorded on a Bruker Vector-22 spectrometer. The pH values of the test solutions were measured with a glass electrode connected to a Mettler-Toledo Instruments DELTA 320 pH meter (Shanghai, China) and adjusted if necessary. Fluorescence spectra were determined on a Hitachi F-4500. UV-Vis spectra were recorded on a Hitachi U-3010 UV-Vis spec.

3. Synthesis

3.1 Synthesis of intermediate (1)

To a solution of aniline (5 mL, 0.05 mol) in a small quantity of water was slowly added 20 mL of 50% HCl solution at 0–5 °C with stirring. Then, the solution of $NaNO_2$ (4 g $NaNO_2$ + 20 mL H_2O) was added to the above-mentioned mixture and the resulting solution was stirred for 1 h to give a bright yellow solution. Salicylaldehyde (5 mL, 0.05 mol) was dissolved in the solution of Na_2CO_3 (18 g Na_2CO_3 + 120 mol H_2O). Then the solution of salicylaldehyde was added dropwise to the bright yellow solution for 1 h. After stirring for 4 h, the reaction mixture was neutralized with HCl, the brown crude solid was filtered and recrystallized from ethanol to afford a pure yellow product. Yield: 62.8%.

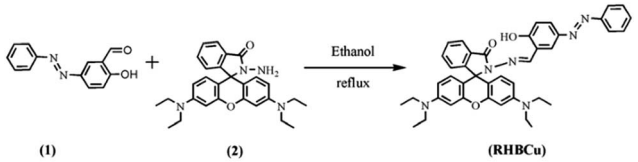

Scheme 1 Synthesis and structure of sensor 1.

3.2 Synthesis of intermediate (2)

Rhodamine B (5.0 g, 10.46 mmol) was dissolved in 150 mL of anhydrous ethanol; 10 mL (excess) hydrazine hydrate (85%) was then added. After the addition, the stirred mixture was heated to reflux in an air bath for 2 h. The solvent was evaporated under reduced pressure, 1 M NaOH was added slowly with stirring until the pH of the solution reached.[30,31] The resulting precipitate was filtered and washed 3 times with water. The crude material was purified by flash column chromatography to give white product RHB-hydrazine (CH_2Cl_2/EtOH/Et_3N, 5 : 1 : 0.1), yield: 50.8%.

3.3 Synthesis of sensor 1

To 30 mL anhydrous ethanol containing (2) (0.50 g, 1.1 mmol), an excessive (1) (0.34 g, 1.5 mmol) was added and the mixture was stirred vigorously at 90 °C for 24 h. After completion of the reaction, the formed precipitate was filtered, washed with cold ethanol (3 × 10 mL) and then dried in vacuum, affording 0.65 g crude product, which was purified by flash column chromatography to give white product RHB-hydrazine. (CH_2Cl_2/EtOH/Et_3N, 5 : 1 : 0.1), yield: 75.6%. ^{1}H NMR (300 MHz, $CDCl_3$, δ): 8.06 (d, J = 7.6 Hz, 6H), 7.89 (s, 7H), 7.86 (d, J = 2.2 Hz, 7H), 7.80 (s, 5H), 7.60 (d, J = 5.1 Hz, 10H), 7.52 (d, J = 7.7 Hz, 8H), 7.48 (d, J = 6.9 Hz, 5H), 7.28–7.17 (m, 6H), 7.02 (d, J = 8.7 Hz, 6H), 6.56 (s, 19H), 6.35 (s, 10H), 3.39 (d, J = 7.0 Hz, 40H), 1.33–1.12 (m, 59H); ^{13}C NMR (300 MHz, $CDCl_3$, δ): 168.67, 159.93, 152.70, 151.89, 151.09, 148.56, 146.93, 145.00, 134.01, 130.81, 129.29, 128.85, 128.48, 127.57, 125.42, 123.83, 123.34, 123.06, 122.17, 120.06, 117.28, 108.19, 104.91, 97.42, 65.54, 43.61, 12.27; IR (KBr, cm^{-1}): ν = 3437, 2972, 2929, 2893, 1692, 1615, 1548, 1515, 1481, 1466, 1428, 1401, 4135, 1375, 1307, 1267, 1220, 1120, 1079, 814, 788, 769, 759, 700 and 690; HRMS (ESI, m/z): $[M + H]^+$ cal. Cu for $C_{41}H_{40}N_6O_3$, 664.3162; found, 665.3459.

4. Results and discussion

4.1 pH-titration and spectral responses

The effects of pH on the absorption of sensor 1 in the absence and presence of Cu^{2+} are determined over the range 4–14. The pH dependence of absorption spectra is shown in Fig. 1 and 2. As we can see the sensor and the complex are stable in the wide range of pH 4–10, suggesting that it could be used for the estimation of Cu^{2+} under complex physiological conditions for biological applications.

4.2 Cu^{2+}-titration and spectral responses

In order to gain an insight into the signalling properties of the sensor 1 toward Cu^{2+}, fluorescence titration was conducted. Fluorescence titration of the sensor 1 was investigated in ethanol–water (1 : 10, v/v) solution ($[Cu^{2+}] = 2.0 \times 10^{-6}$ mol L^{-1},

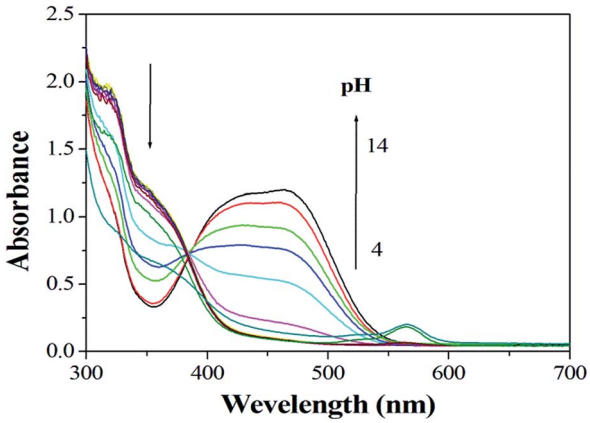

Fig. 1 Absorption of sensor 1 with different pH.

Fig. 2 Color changes of sensor 1 in ethanol–water (1 : 10, v/v) measured as a function of pH.

0.1 M Tris–HCl buffer at pH = 7.14, λ_{ex} = 500 nm, λ_{em} = 565 nm). Upon addition of Cu^{2+}, about a 14-fold increase in fluorescence intensity was observed at 575 nm (Fig. 3). When more than 1.0 equiv. Cu^{2+} was added, the maximum fluorescence intensity was

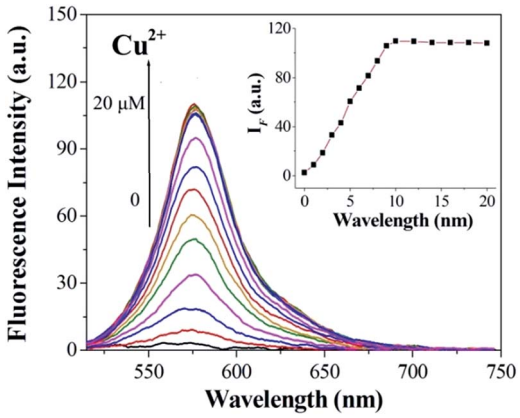

Fig. 3 The fluorescence intensity change profile of sensor 1 (1 μM) to different metal ions (1 mM) in 0.1 M Tris–HCl solution (ethanol–water = 1 : 10, v/v, pH 7.14, λ_{ex} = 500 nm). Inset: corresponding fluorescent spectra of 1 in the presence of different concentrations Cu^{2+} ions.

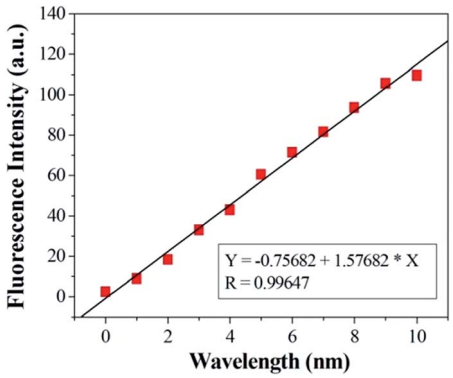

Fig. 4 Curve of fluorescence intensity at 525 nm of sensor 1 *versus* increasing concentrations of Cu^{2+}.

retained. The reaction responsible for these changes reached completion well within the time frame (<30 s) of the measurement. Significantly, the enhancement of fluorescence intensity of sensor 1 corresponded to the concentration of Cu^{2+} in a linear manner (linearly dependent coefficient: R = 0.9929) (Fig. 4), which indicated that sensor 1 had potential use for the quantitative determination of Cu^{2+}. It should be noted that this switch on sensing process could be readily detected not only by fluorescence spectroscopy but also by the naked eye. Moreover, a Job's plot, which exhibited a maximum at 0.5 mole fraction of sensor 1, indicated the 1 : 1 stoichiometry between Cu^{2+} and sensor 1 (Fig. 5). Therefore, on the basis of 1 : 1 stoichiometry and fluorescence titration data, the detection limit was found to be 7.2×10^{-7} mol L^{-1} (based on S/N = 3).

Fig. 6 shows the result of absorption titration of sensor 1 with Cu^{2+} ions. When no Cu^{2+} ions were added to the solution of sensor 1, free 1, as expected, exhibited almost no absorption near 500–600 nm, indicating that sensor 1 exists as a spirocyclic form. Upon addition of increasing concentrations of Cu^{2+} ions to the solution, two absorption bands centered at 380 nm and 560 nm appeared with increasing intensity, which can be ascribed to the formation of the ring-opened amide form of sensor 1 upon Cu^{2+} ions binding. Moreover, the titration solution exhibited an obvious and characteristic colour change from

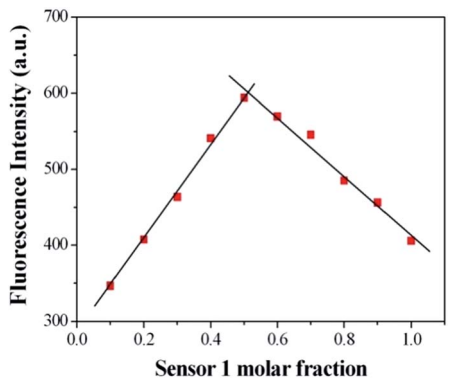

Fig. 5 Job's plot for sensor 1 (forms 1 : 1 complexes) in 0.1 M Tris–HCl solution (ethanol–water = 1 : 10, v/v, pH = 7.14). The total concentration of sensor 1 and Cu^{2+} is 2 μM.

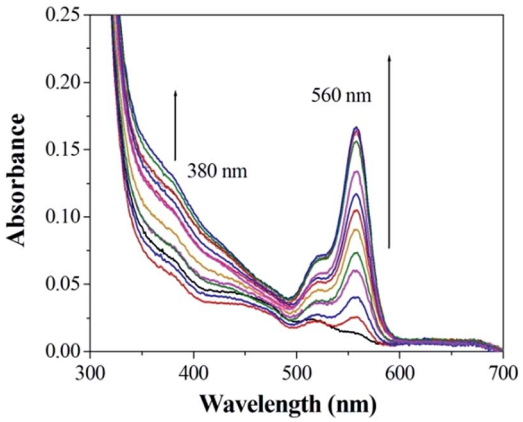

Fig. 6 The absorption change profile of sensor 1 (1 μM) to different metal ions (2 mM) in 0.1 M Tris–HCl solution (ethanol–water = 1 : 10, v/v, pH 7.14).

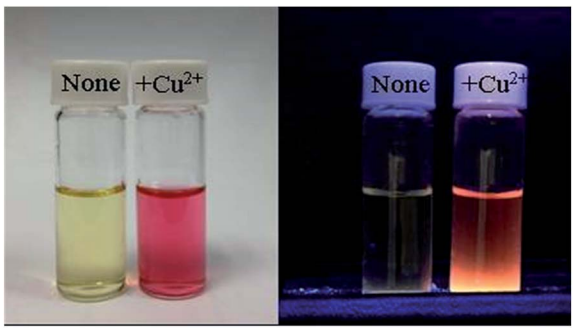

Fig. 7 Change in color (left) and fluorescence (right) of sensor 1 (10 mM) in buffered (Tris–HCl, pH 7.14, ethanol–water = 1 : 10, v/v) upon addition of 1 mM Cu^{2+} ions.

colourless to red (Fig. 7), suggesting that sensor 1 can serve as a "naked-eye" indicator for Cu^{2+} ions.

4.3 Response of sensor 1 to various metal ions and competition experiments

Other representative metal ions, such as Na^{+}, K^{+}, Ca^{2+}, Mg^{2+}, Mn^{2+}, Ni^{2+}, Fe^{3+}, Hg^{2+}, Co^{2+}, Pb^{2+}, Zn^{2+} ions, showed almost

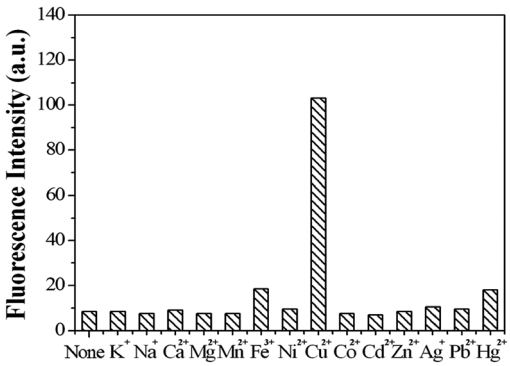

Fig. 8 The fluorescence intensity of sensor 1 (1 μM) in the presence of different metal ions (10 μM).

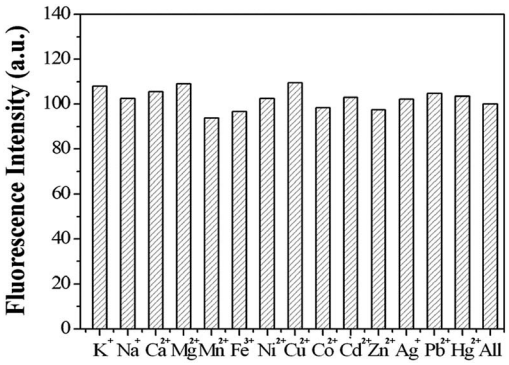

Fig. 9 The fluorescence intensity of sensor 1 (μM) with 1.5 equiv. of Cu^{2+}, followed by 10 equiv. of M^{n+}. (Tris–HCl, pH 7.14, ethanol–water = 1 : 10, v/v, λ_{ex} = 500 nm).

Fig. 10 Images of HeLa cells. (a) Bright fields image of HeLa cells incubated sensor 1; (b) fluorescence image of (a); (c) fluorescence image of HeLa cells incubated with sensor 1 and Cu^{2+}.

negligible effects on the fluorescence behavior of sensor 1 (Fig. 8). In order to further test the interference of other common cations in the determination of Cu^{2+}, competition experiments were performed in which the fluorescent sensor was added to a solution of Cu^{2+} in the presence of other metal ions (Fig. 9). The competition experiments were conducted in the presence of Cu^{2+} ion mixed with Na^{+}, K^{+}, Ca^{2+}, Mg^{2+}, Mn^{2+}, Ni^{2+}, Fe^{3+}, Hg^{2+}, Co^{2+}, Pb^{2+}, Zn^{2+}, respectively. Experimental results indicated that these ions showed no obvious interference in the Cu^{2+} detection. Thus, the sensor 1 exhibited excellent selectivity toward Cu^{2+}, which its practical application.

4.4 Potential application of sensor 1 for Cu^{2+} fluorescence imaging in HeLa cells

To investigate the potential biological application of sensor 1, fluorescence imaging experiments were attempted on HeLa cells (Fig. 10). The cells were incubated with 10 μM of sensor 1 for 30 min at 37 °C, only slightly fluorescence was observed owing to a small quantity of Cu^{2+} in cancer cells (Fig. 10b), which was confirmed by previous research.[32–34] However, the cells were added with 20 μM of Cu^{2+} for another 30 min, an obviously fluorescence response was observed (Fig. 10c). The fluorescence imaging experiments confirmed that sensor 1 had good cell-permeability and could be used for detecting Cu^{2+} in living cells.

5. Conclusions

In conclusion, we have synthesized a simple and easy-to-prepare azo-phenol derivative optical chemosensor 1 for the

detection of Cu^{2+} ions. The chemosensor 1 displayed 1 : 1 complex formation with Cu^{2+} ions. Cu^{2+}-specific binding enabled the opening of the spirolactam ring and consequently successfully exhibited a obvious absorption and fluorescence enhancement response toward Cu^{2+} ions over other metal ions. Thus the chemosensor 1 behaves as a highly sensitive and selective fluorescent probe for Cu^{2+} ions detection. Moreover, we have demonstrated the application of sensor 1 by imaging intracellular Cu^{2+} in HeLa cells, which demonstrated the potentialvalue in living system.

Acknowledgements

This work was supported by the Scientific and Technological Development Plan Project of Jilin Province (Grant No. 20160101311JC).

Notes and references

1 K. C. Jones, *Environ. Pollut.*, 1993, **81**, 301.
2 C. C. Bridges and R. K. Zalups, *Toxicol. Appl. Pharmacol.*, 2005, **204**, 274–308.
3 J. H. Lee and G. F. Birch, *Environ. Monit. Assess.*, 2016, **188**, 1–17.
4 J. Tian, Q. Liu, A. M. Asiri, A. O. Al-Youbi and X. Sun, *Anal. Chem.*, 2013, **85**, 5595–5599.
5 W. Lu, X. Qin, S. Liu, G. Chang, Y. Zhang, Y. Luo, A. M. Asiri, A. O. Al-Youbi and X. Sun, *Anal. Chem.*, 2012, **84**, 5351–5357.
6 L. Zeng, E. W. Miller, A. Pralle, E. Y. Isacoff and C. J. Chang, *J. Am. Chem. Soc.*, 2010, **128**, 10–11.
7 S. P. Wu, Z. M. Huang, S. R. Liu and P. K. Chung, *J. Fluoresc.*, 2012, **23**, 1139–1145.
8 B. Sen, M. Mukherjee, S. Pal, S. Sen and P. Chattopadhyay, *RSC Adv.*, 2015, **5**, 50532–50539.
9 P. Chattopadhyay, B. Sen, M. Mukherjee, S. Pal and S. Sen, *RSC Adv.*, 2015, **5**, 50532–50539.
10 M. Yang, H. Wang, J. Huang, M. Fang, B. Mei, H. Zhou, J. Wu and Y. Tian, *Sens. Actuators, B*, 2014, **204**, 710–715.
11 Y. Wang, H. Q. Chang, W. N. Wu, X. J. Mao, X. L. Zhao, Y. Yang, Z. Q. Xu, Z. H. Xu and L. Jia, *J. Photochem. Photobiol., A*, 2017, **335**, 10–16.
12 X. Wang, J. Zhao, C. Guo, M. Pei and G. Zhang, *Sens. Actuators, B*, 2014, **193**, 157–165.
13 S. Li and S. Dong, *J. Mater. Chem.*, 2008, **18**, 4636–4640.
14 Q. Qu, A. Zhu, X. Shao, G. Shi and Y. Tian, *Chem. Commun.*, 2012, **48**, 5473–5475.
15 M. Yu, M. Shi, Z. Chen, F. Li, X. Li, Y. Gao, J. Xu, H. Yang, Z. Zhou and T. Yi, *Chemistry*, 2008, **14**, 6892–6900.
16 W. Wang, Q. Yang, L. Sun, H. Wang, C. Zhang, X. Fei, M. Sun and Y. Li, *J. Hazard. Mater.*, 2011, **194**, 185–192.
17 X. Q. Chen, T. Pradhan, F. Wang, J. S. Kim and J. Yoon, *Chem. Rev.*, 2012, **112**, 1910–1956.
18 X. Zhang, X. J. Huang and Z. J. Zhu, *RSC Adv.*, 2013, **3**, 24891–24895.
19 A. Dhara, A. Jana, N. Guchhait, P. Ghosh and S. K. Kar, *New J. Chem.*, 2014, **38**, 1627–1634.
20 Y. Zhou, F. Wang, Y. Kim, S.-J. Kim and J. Yoon, *Org. Lett.*, 2009, **11**, 4442–4445.
21 Z. Xu, L. Zhang, R. Guo, T. Xiang, C. Wu, Z. Zheng and F. Yang, *Sens. Actuators, B*, 2011, **156**, 546–552.
22 C. Yu, J. Zhang, R. Wang and L. Chen, *Org. Biomol. Chem.*, 2010, **8**, 5277–5279.
23 Y. Zhao, X.-B. Zhang, Z.-X. Han, L. Qiao, C.-Y. Li, Li-X. Jian, G.-L. Shen and R.-Q. Yu, *Anal. Chem.*, 2009, **81**, 7022–7030.
24 Y. X. Wu, J. B. Li, L. H. Liang, D. Q. Lu, J. Zhang, G. J. Mao, L. Y. Zhou, X. B. Zhang, W. H. Tan, G. L. Shen and R. Q. Yu, *Chem. Commun.*, 2014, **50**, 2040–2042.
25 Y. Yuan, S. G. Sun, S. Liu, X. W. Song and X. J. Peng, *J. Mater. Chem. B*, 2015, **3**, 5261–5265.
26 B. Zhu, C. Gao, Y. Zhao, C. Liu, Y. Li, Q. Wei, Z. Ma, B. Du and X. Zhang, *Chem. Commun.*, 2011, **47**, 8656.
27 L. M. Zhang, L. E. Guo, X. M. Li, Y. G. Shi, G. F. Wu, X. G. Xie, Y. Zhou, Q. H. Zhao and J. F. Zhang, *Tetrahedron Lett.*, 2014, **55**, 6131–6136.
28 J. F. Zhang, S. Kim, J. H. Han, S. J. Lee, T. Pradhan, Q. Y. Cao, C. Kang and J. S. Kim, *Org. Lett.*, 2011, **13**, 5294–5297.
29 M. R. Maurya, S. J. J. Titinchi and S. Chand, *J. Mol. Catal. A: Chem.*, 2003, **193**, 165–176.
30 H. Yang, Z. Zhou, K. Huang, M. Yu, F. Li, T. Yi and C. Huang, *Org. Lett.*, 2007, **9**, 4729–4732.
31 H. S. Jung, P. S. Kwon, J. W. Lee, J. I. Kim, S. H. Chang, J. W. Kim, S. Yan, Y. L. Jin, J. H. Lee and T. Joo, *J. Am. Chem. Soc.*, 2009, **131**, 2008–2012.
32 M. C. Linder and M. Hazegh-Azam, *Am. J. Clin. Nutr.*, 1996, **63**, 797S–811S.
33 D. Chen, Q. C. Cui, H. Yang, R. A. Barrea, F. H. Sarkar, S. Sheng, B. Yan, G. P. Reddy and Q. P. Dou, *Cancer Res.*, 2007, **67**, 1636–1644.
34 R. An, D. Zhang, Y. Chen and Y.-Z. Cui, *Sens. Actuators, B*, 2016, **222**, 48–54.